

The reverse Warburg effect

Glycolysis inhibitors prevent the tumor promoting effects of caveolin-1 deficient cancer associated fibroblasts

Gloria Bonuccelli,^{1,2} Diana Whitaker-Menezes,^{1,2} Remedios Castello-Cros,^{1,2} Stephanos Pavlides,^{1,2} Richard G. Pestell,^{1,2} Alessandro Fatatis,³ Agnieszka K. Witkiewicz,⁴ Matthew G. Vander Heiden,⁵ Gemma Migneco,^{1,2} Barbara Chiavarina,^{1,2} Philippe G. Frank,^{1,2} Franco Capozza,^{1,2} Neal Flomenberg,⁶ Ubaldo E. Martinez-Outschoorn,^{1,2,6} Federica Sotgia^{1,2,*} and Michael P. Lisanti^{1,2,6,*}

¹Departments of Stem Cell Biology and Regenerative Medicine; and Cancer Biology; ²The Jefferson Stem Cell Biology and Regenerative Medicine Center; ³Department of Pathology, Anatomy and Cell Biology; and ⁴Department of Medical Oncology; Kimmel Cancer Center; Thomas Jefferson University; Philadelphia, PA USA; ⁵Departments of Pharmacology and Physiology; and Pathology and Laboratory Medicine; Drexel University College of Medicine; Philadelphia, PA USA; ⁶Koch Institute for Integrative Cancer Research at MIT; Cambridge, MA USA

Key words: caveolin-1, tumor stroma, myofibroblast, cancer associated fibroblast, aerobic glycolysis, M2-isoform of pyruvate kinase, lactate dehydrogenase, Warburg effect

We and others have previously identified a loss of stromal caveolin-1 (Cav-1) in cancer-associated fibroblasts (CAFs) as a powerful single independent predictor of breast cancer patient tumor recurrence, metastasis, tamoxifen-resistance and poor clinical outcome. However, it remains unknown how loss of stromal Cav-1 mediates these effects clinically. To mechanistically address this issue, we have now generated a novel human tumor xenograft model. In this two-component system, nude mice are co-injected with (1) human breast cancer cells (MDA-MB-231), and (2) stromal fibroblasts [wild-type (WT) versus Cav-1 (-/-) deficient]. This allowed us to directly evaluate the effects of a Cav-1 deficiency solely in the tumor stromal compartment. Here, we show that Cav-1-deficient stromal fibroblasts are sufficient to promote both tumor growth and angiogenesis, and to recruit Cav-1 (+) micro-vascular cells. Proteomic analysis of Cav-1-deficient stromal fibroblasts indicates that these cells upregulate the expression of glycolytic enzymes, a hallmark of aerobic glycolysis (the Warburg effect). Thus, Cav-1-deficient stromal fibroblasts may contribute towards tumor growth and angiogenesis, by providing energy-rich metabolites in a paracrine fashion. We have previously termed this new idea the "Reverse Warburg Effect." In direct support of this notion, treatment of this xenograft model with glycolysis inhibitors functionally blocks the positive effects of Cav-1-deficient stromal fibroblasts on breast cancer tumor growth. Thus, pharmacologically-induced metabolic restriction (via treatment with glycolysis inhibitors) may be a promising new therapeutic strategy for breast cancer patients that lack stromal Cav-1 expression. We also identify the stromal expression of PKM2 and LDH-B as new candidate biomarkers for the "Reverse Warburg Effect" or "Stromal-Epithelial Metabolic Coupling" in human breast cancers.

It is becoming increasingly clear that the tumor microenvironment plays a critical role in determining tumor recurrence, metastasis, drug-resistance and overall clinical outcome, in many different types of epithelial cancers, including breast cancer.^{1,2} In accordance with this idea, we have recently identified the loss of expression of caveolin-1 (Cav-1) in stromal cancer-associated fibroblasts³ as a new prognostic biomarker for breast cancers.⁴

In a well-annotated cohort of 160 breast cancer patients, a loss of stromal Cav-1 in cancer-associated fibroblasts was associated with a dramatically increased risk of tumor recurrence, lymph node metastasis, tamoxifen-resistance, and poor clinical outcome.⁵ Interestingly, the predictive value of stromal Cav-1 in this patient population was independent of tumor epithelial marker status (ER, PR, HER2), indicating that it may be beneficial in

all the different sub-types of human breast cancers, including triple-negative patients.⁵ Virtually identical conclusions were also reached independently by another laboratory, using a different Cav-1 antibody probe, and a second independent breast cancer patient cohort.⁶

Stromal Cav-1 levels were also used to predict DCIS recurrence and progression to invasive breast cancer in a patient population with nearly 20 years of follow-up data.⁷ In this data set, 100% of the patients with a loss of stromal Cav-1 had a recurrence, and 80% of these patients progressed to invasive breast cancer.⁷ Finally, similar results were obtained using a prostate cancer patient cohort. In these patients, a loss of stromal Cav-1 expression was strictly associated with advanced prostate cancer, disease progression, and metastasis (both local and distant).⁸

*Correspondence to: Federica Sotgia and Michael P. Lisanti; Email: federica.sotgia@jefferson.edu and michael.lisanti@kimmelcancercenter.org
Submitted: 02/19/10; Accepted: 02/23/10
Previously published online: www.landesbioscience.com/journals/cc/article/11601

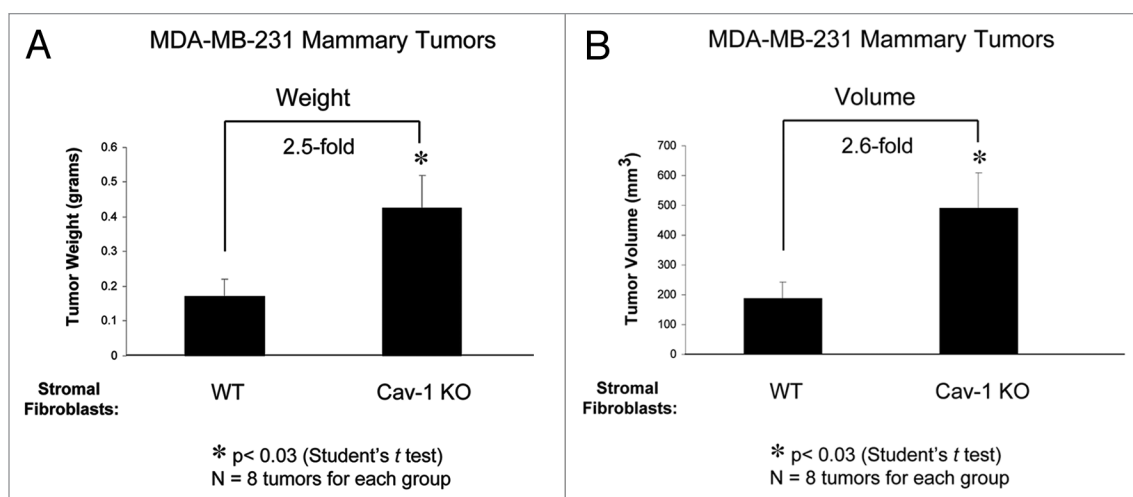


Figure 1. Cav-1 deficient stromal fibroblasts drive breast cancer tumor growth. To determine if loss of Cav-1 in the fibroblast compartment is sufficient to confer the cancer-associated fibroblast phenotype, we developed a novel xenograft model. v-Src-immortalized stromal fibroblasts [WT vs. Cav-1 (-/-)] were co-injected with a human breast cancer cell line (MDA-MB-231 cells) in the flanks of nude mice. After 2 weeks, the tumors that formed were harvested and subjected to a detailed analysis. Note that co-injection with Cav-1-deficient stromal fibroblasts promoted the growth of MDA-MB-231 derived tumors by at least 2.5-fold. WT, tumors grown with Cav-1 (+/+) fibroblasts; Cav-1 KO, tumors grown with Cav-1 (-/-) fibroblasts. (A) tumor weight; (B) tumor volume.

Thus, a loss of stromal Cav-1 may be involved mechanistically in all the different phases of epithelial tumorigenesis, including cancer initiation, progression and metastasis.⁴

In order to begin to dissect the molecular mechanism(s) underlying the strong prognostic value of a loss of stromal Cav-1, we have used Cav-1 (-/-) deficient mice as a model system.^{9,10} Importantly, mammary fibroblasts derived from Cav-1 (-/-) deficient mice share many properties with authentic human breast cancer-associated fibroblasts, including (1) hyper-proliferation, (2) the secretion of pro-tumorigenic, pro-angiogenic, and pro-inflammatory growth factors and (3) the onset of a myofibroblastic phenotype, with overexpression of alpha-smooth muscle actin (SMA), and constitutive activation of TGFbeta signaling.¹⁰

Interestingly, “conditioned media” derived from Cav-1 (-/-) deficient fibroblasts is sufficient to induce normal mammary epithelial cells to undergo an epithelia-mesenchymal transition (EMT), indicative of a more motile and invasive phenotype.¹⁰

However, it remains unknown if Cav-1 (-/-) deficient stromal fibroblasts are sufficient to promote tumorigenesis in vivo. To address this issue directly, we have developed a new xenograft-based model system employing (1) human breast cancer cells (MDA-MB-231 cells) and (2) immortalized Cav-1 (-/-) deficient fibroblasts. Our results directly show that Cav-1 (-/-) deficient fibroblasts promote tumor growth, as well as tumor angiogenesis, by recruiting Cav-1 (+) microvascular cells from the host.

Furthermore, unbiased proteomic analysis of primary cultures of Cav-1 (-/-) deficient stromal cells mechanistically identified a shift towards aerobic glycolysis (a.k.a., the Warburg effect) in the fibroblastic tumor stromal compartment.¹¹ We have previously termed this new idea the “Reverse Warburg Effect,”¹¹ because the “Warburg effect” was previously thought to be confined to epithelial cancer cells, and not to the tumor stroma. In accordance with these findings, here we show that energy restriction with

glycolysis inhibitors (2-DG and DCA) is sufficient to block tumor growth stimulated by Cav-1 (-/-) deficient stromal fibroblasts.

Finally, we demonstrate that glycolytic enzymes (such as PKM2 and LDH-B) are selectively upregulated in the fibroblastic stromal compartment of human breast cancer samples that lack stromal Cav-1 expression. Thus, stromal PKM2 and LDH-B may be novel biomarkers for the “Reverse Warburg Effect,” allowing the stratification and selection of breast cancer patients for metabolic-based therapies.

Results

Cav-1 deficient stromal fibroblasts drive tumor growth and angiogenesis. In order to determine if loss of Cav-1 in the fibroblast compartment is sufficient to confer the cancer-associated fibroblast phenotype, we developed a two-component system using a novel xenograft model. Briefly, immortalized stromal fibroblasts [WT vs. Cav-1 (-/-)] were co-injected with a human breast cancer cell line (MDA-MB-231 cells) in the flanks of nude mice. After 2 weeks, the tumors that formed were harvested and subjected to a detailed analysis.

Remarkably, **Figure 1** shows that co-injection with Cav-1-deficient stromal fibroblasts promoted the growth of MDA-MB-231 derived tumors by at least 2.5-fold. Thus, Cav-1-deficient stromal fibroblasts are indeed sufficient to promote breast cancer tumor growth in an in vivo setting.

To determine if this increase in tumor growth was associated with augmented neo-vascularization/angiogenesis, frozen-sections prepared from these tumor samples were immunostained with antibodies directed against CD31 (a.k.a., PECAM1), a well-established marker of the microvasculature. **Figure 2** directly shows that the breast tumors formed employing Cav-1-deficient stromal fibroblasts were highly vascularized, as predicted. Several

representative images are shown. Importantly, quantitation revealed a >3-fold increase in both vessel area and vessel number (Fig. 3A and B).

To determine if these tumor vessels were derived directly from Cav-1-deficient stromal cells, or via the recruitment of endothelial progenitor cells from the host, we next immuno-stained these breast cancer derived tumors with antibodies to Cav-1. Figure 4 shows that the vasculature associated with breast tumors grown using Cav-1-deficient stromal fibroblasts were prominently stained with antibodies to Cav-1. Thus, Cav-1-deficient stromal fibroblasts functionally recruit Cav-1-positive endothelial cells or progenitors from the host, in order to sustain tumor growth.

Importantly, virtually identical results were also obtained with MDA-MB-231 cells engineered to overexpress GFP (Fig. 5A and B). Using MDA-MB-231 (GFP⁺) cells, Cav-1-deficient stromal fibroblasts efficiently promoted tumor growth (Fig. 5A), by nearly 2-fold, and also promoted angiogenesis (Fig. 5B). These results also directly show that the bulk of these breast cancer derived tumors consist of MDA-MB-231 (GFP⁺) cells, surrounded by tumor vasculature.

Proteomic analysis of Cav-1 deficient stromal fibroblasts reveals a shift towards aerobic glycolysis. In order to dissect the mechanism by which Cav-1-deficient stromal cells promote tumor growth and angiogenesis, we subjected cell lysates and conditioned media derived from these cells to an unbiased proteomics analysis using 2-D DIGE (two-dimensional difference gel electrophoresis; See Materials and Methods for specific details). See also Supplemental Figures 1 and 2 for representative 2-D gel analysis.

A detailed summary of this unbiased proteomics analysis is presented in Table 1. Interestingly, Cav-1-deficient stromal fibroblasts show the upregulation of a number of (1) myo-fibroblast markers (such as calponin, and tropomyosin), (2) extracellular matrix proteins (including PAI2, collagen-3, and galectin-1), and (3) glycolytic enzymes [such as pyruvate kinase (M2-isoform), lactate dehydrogenase A/C, and aldolase A]. Importantly, our proteomic studies using Cav-1 (-/-) null fibroblasts

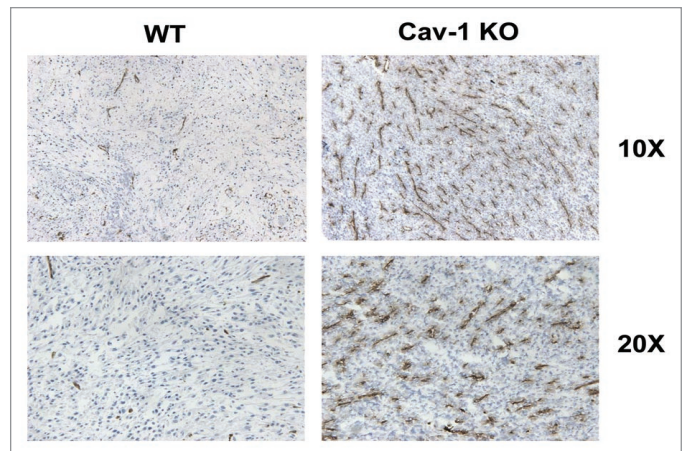


Figure 2. Cav-1 deficient stromal fibroblasts promote tumor angiogenesis: CD31 Immuno-staining. To determine if the increase in tumor growth was associated with augmented neo-vascularization/angiogenesis, frozen-sections prepared from these tumor samples were immuno-stained with antibodies directed against CD31 (a.k.a., PECAM1). Note that breast tumors formed employing Cav-1-deficient stromal fibroblasts were highly vascularized, as predicted. Several representative images are shown.

cells detected a peptide specific for the murine M2-isoform (EAEAAIYHLQLFEELRR), but not the corresponding peptide expected from the M1-isoform. The upregulation of glycolytic enzymes is characteristic of the Warburg effect. This suggests that Cav-1-deficient stromal fibroblasts are undergoing a shift towards aerobic glycolysis. This would presumably result in more secreted lactate and pyruvate, that could directly contribute metabolic energy for tumor growth and tumor angiogenesis, but in a paracrine fashion. In support of this idea, Cav-1-deficient stromal fibroblasts also show an increase in the expression of uridine phosphorylase 1 (part of the uridine salvage pathway for nucleotide biosynthesis), which is characteristic of mammalian cells with defective oxidative phosphorylation, due to mitochondrial depletion/malfunction.¹²

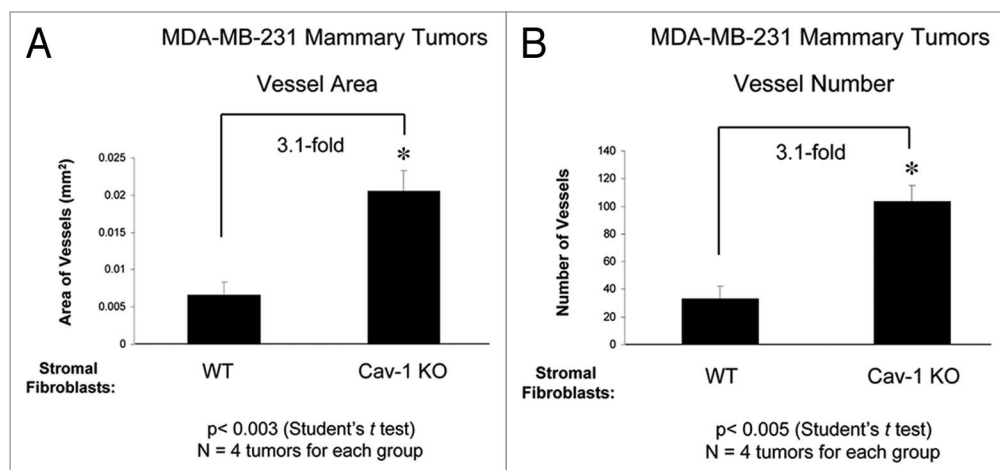


Figure 3. Cav-1 deficient stromal fibroblasts promote tumor angiogenesis. Vessel area (A) and vessel number (B) is presented. Note the >3-fold increase in both vessel area and vessel number.

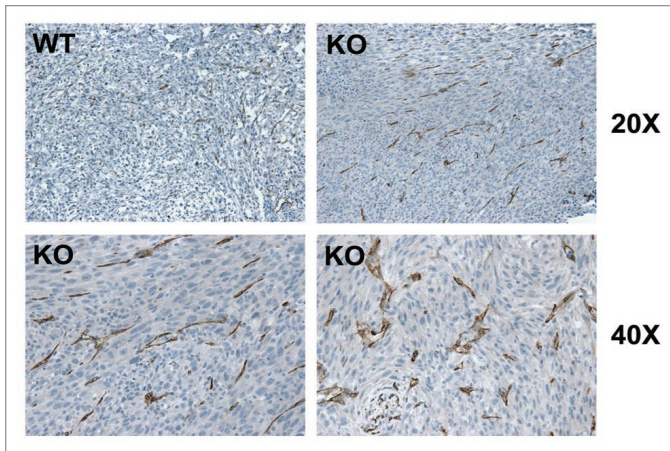


Figure 4. Cav-1 deficient stromal fibroblasts recruit Cav-1-positive vascular cells to the tumor. To determine if the tumor vessels were derived directly from Cav-1-deficient stromal cells, or via the recruitment of endothelial progenitor cells from the host, we next immuno-stained these breast cancer derived tumors with antibodies to Cav-1. Note that the vasculature associated with breast tumors grown with Cav-1-deficient stromal fibroblasts was prominently stained with antibodies to Cav-1. As such, it appears that Cav-1-deficient stromal fibroblasts functionally recruit Cav-1-positive endothelial cells or progenitors from the host. WT, tumors grown with Cav-1 (+/+) fibroblasts; KO, tumors grown with Cav-1 (-/-) fibroblasts.

We also validated the overexpression of PKM2 and LDH isoforms in Cav-1-deficient stromal fibroblasts by Western blot analysis, using either cell lysates or conditioned media. **Figure 6** directly shows that PKM2 and LDH isoforms are either overexpressed in or secreted from Cav-1-deficient stromal fibroblasts, consistent with our unbiased proteomics analysis. Both of these fibroblast lines fail to express detectable levels of PKM1.

Interestingly, a decrease in stromal fibulin-2 and an increase in stromal galectin-1 (as we see in **Table 1**) have been previously associated with poor clinical outcome in human breast cancer patients.¹³⁻¹⁵

Treatment with glycolysis inhibitors functionally blocks cancer-associated fibroblast induced breast cancer tumor growth. In summary, our unbiased proteomics analysis of Cav-1-deficient stromal fibroblasts identified the Warburg effect (aerobic glycolysis) in the tumor stromal compartment. Thus, the Warburg effect, in the myo-fibroblast compartment, may be a key factor driving tumor growth.

To test this hypothesis directly, mice co-injected with Cav-1-deficient stromal fibroblasts and MDA-MB-231 breast cancer cells were treated with glycolysis inhibitors. For this purpose, we tested the efficacy of two well-established glycolysis inhibitors, namely 2-DG (2-deoxy-D-glucose) and DCA (dichloro-acetate), individually or in combination. Interestingly, individually 2-DG or DCA had no effect on tumor growth at a dosage of 200 mg/kg (data not shown). However, 2-DG and DCA, used in combination, dramatically reduced tumor growth that was dependent on Cav-1-deficient stromal fibroblasts. Under these conditions, we observed a striking 4.5-fold reduction in tumor mass (**Fig. 7**).

Validation studies employing the immuno-histochemical staining of human breast cancers that lack stromal Cav-1. To validate the potential clinical relevance of our proteomic findings for human breast cancers (**Table 1**), we immuno-stained sections from human breast cancer tumor tissues that were pre-selected based on a lack of stromal expression of Cav-1. Using this immuno-histochemical approach, we directly validated the tumor stromal expression of several extracellular matrix proteins (galectin-1 and collagen-3) (**Fig. 8**), as well as multiple glycolytic enzymes (pyruvate kinase, M2 isoform; lactate dehydrogenase, isoforms A, B and C) (**Figs. 9-12**).

Figures 9 and 10 directly show that M2-pyruvate kinase, the key glycolytic enzyme

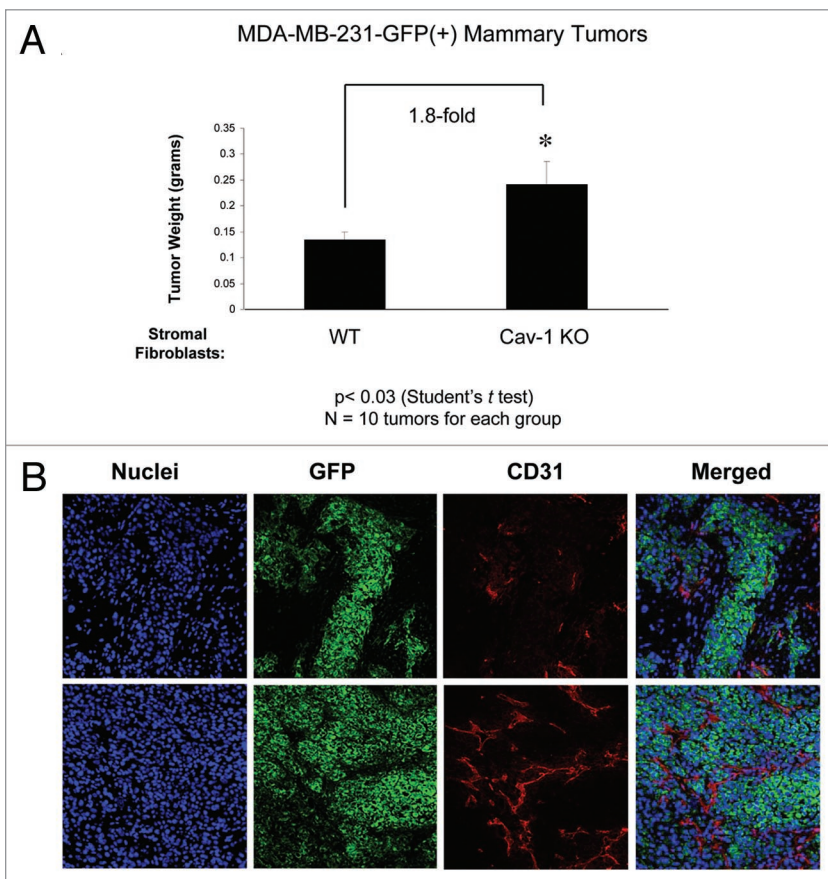


Figure 5. Tumor epithelial cells visualized with GFP constitute the bulk of the tumor mass. (A) Quantitation of Tumor Growth; (B) Fluorescence Imaging. Using MDA-MB-231 (GFP⁺) cells, Cav-1-deficient stromal fibroblasts efficiently promoted tumor growth (A), by nearly two-fold, and also promoted angiogenesis (B). These results also directly show that the bulk of these breast cancer derived tumors consist of MDA-MB-231 (GFP⁺) cells, surrounded by tumor vasculature.

Table 1. Proteomic analysis of WT and Cav-1 (-/-) stromal cells [mouse embryo fibroblasts (MEFs)]

Name	Accession #	Spot #	Fold-change (KO/WT)
Muscle and Myo-fibroblast Related Proteins			
calponin 2	gi 6680952	32; CL	4.1
gamma-actin	gi 809561	41; CM	3.5
gelsolin-like capping protein	gi 110227377	43; CM	2.9
alpha-tropomyosin	gi 157787199	27; CL	2.9
Epithelial Keratins			
Keratin 8	gi 76779293	11; CL	-10.2
Keratin 8	gi 76779293	10; CL	-6.5
Signaling Molecules			
Rho, GDP dissociation inhibitor (GDI) beta	gi 33563236	42; CL	10.1
cellular retinoic acid binding protein II	gi 33469075	55; CL	9.7
retinol binding protein 1, cellular	gi 6755300	54; CL	-3.8
caspase 3	gi 6753284	35; CL	-2.6
Glycolytic Enzymes and the Pentose Phosphate Pathway			
pyruvate kinase, muscle	gi 31981562	22; CM	9.7
pyruvate kinase M2	gi 551295	21; CM	7.7
pyruvate kinase, muscle	gi 31981562	18; CM	6.2
pyruvate kinase M2	gi 551295	23; CM	4.1
pyruvate kinase, muscle	gi 31981562	19; CM	3.1
aldolase A	gi 7548322	36; CM	4.1
aldolase A	gi 7548322	37; CM	3.4
L-lactate dehydrogenase A	gi 6754524	57; CM	4.2
L-lactate dehydrogenase C	gi 7305229	55; CM	3.4
6-phosphogluconate dehydrogenase (Pgd)	gi 15990384	33; CM	2.8
Extracellular Matrix Proteins			
serine (or cysteine) proteinase inhibitor, clade b, member 2 (PAI2)	gi 6755098	38; CM	9.6
serine (or cysteine) proteinase inhibitor, clade b, member 2 (PAI2)	gi 6755098	18; CL	8.9
Col3a1 protein	gi 20380522	49; CM	3.2
lectin, galactose binding, soluble 1; galectin-1	gi 6678682	84; CM	3.4
fibulin 2, isoform A	gi 148666878	2; CM	-2.5
Other Secreted Proteins			
fatty acid binding protein 5, epidermal	gi 6754450	87; CM	4.9
fatty acid binding protein 5, epidermal	gi 6754450	56; CL	2.7
Prolactin-2C4 (Prl2c4); Proliferin-3; Mitogen-regulated protein 3 (Mrp3)	gi 130955	64; CM	2.7
Anti-Oxidants associated with Oxidative Stress			
peroxiredoxin 1	gi 6754976	77; CM	2.3
Gsta4 (glutathione S-transferase alpha 4)	gi 3114387	45; CL	-3.7
Protein Synthesis, Ribosome Assembly and Protein Folding			
Pa2g4 protein (proliferation-associated 2G4, 38 kDa)	gi 116283229	31; CM	3.1
Eef2 protein (eukaryotic translation elongation factor 2)	gi 7546551	39; CL	3.1
Eef2 protein (eukaryotic translation elongation factor 2)	gi 38511951	8; CM	2.8
Pipc; peptidylprolyl isomerase C (cyclophilin C)	gi 1000033	48; CL	2.9
Production of Uracil, ribose-1-phosphate or deoxyribose-1-phosphate (for Nucleotide Synthesis)			
Uridine phosphorylase 1; UrdPase 1; UPase 1	gi 31077161	33; CL	2.6

All peptide sequences used for protein identification correspond to the *Mus musculus* protein product, ruling out contamination by serum proteins. CL, cell lysate; CM, conditioned media. Furthermore, our proteomic studies using Cav-1 (-/-) null stromal cells detected a peptide specific for the murine M2-isoform (EAEAAIYHLQLFEELRR), but not the corresponding peptide expected from the M1-isoform.

Table 1. Proteomic analysis of WT and Cav-1 (-/-) stromal cells [mouse embryo fibroblasts (MEFs)] (continued).

Detoxification of Acetaldehyde			
aldehyde dehydrogenase 3A1	gij163310769	12; CL	-2.9
Protein Degradation			
Proteasome subunit beta type-2; Proteasome component C7-I	gij9910832	72; CM	2.8
Other			
hypothetical protein LOC433182	gij70794816	30; CM	3.9

All peptide sequences used for protein identification correspond to the *Mus musculus* protein product, ruling out contamination by serum proteins. CL, cell lysate; CM, conditioned media. Furthermore, our proteomic studies using Cav-1 (-/-) null stromal cells detected a peptide specific for the murine M2-isoform (EAEAAIYHLQLFEELRR), but not the corresponding peptide expected from the M1-isoform.

involved in conferring the “Warburg Effect,”¹⁶ was abundantly expressed in the tumor stromal compartment, using two distinct isoform-specific antibody probes that specifically recognize the M2-isoform. Interestingly, two different stromal patterns of localization were observed for PKM2, consistent with the idea that M2-pyruvate kinase may be localized within stromal fibroblasts and/or secreted by stromal cells.

In contrast, LDH-A and LDH-C were localized in both the breast cancer tumor epithelial cells and the fibroblastic stromal compartment, with LDH-C showing some preference for the stromal compartment (Fig. 11).

Remarkably, LDH-B was almost solely confined to the fibroblastic tumor stromal compartment (Fig. 12). Thus, LDH-B may be an interesting new candidate tumor stromal biomarker for the “Reverse Warburg Effect,” in addition to PKM2.

Discussion

Recently, we proposed a new model to explain the “Warburg Effect” in tumor metabolism.¹¹ In this scenario, we suggested that epithelial cancer cells would induce the Warburg effect in adjacent cancer-associated fibroblasts, via the downregulation of

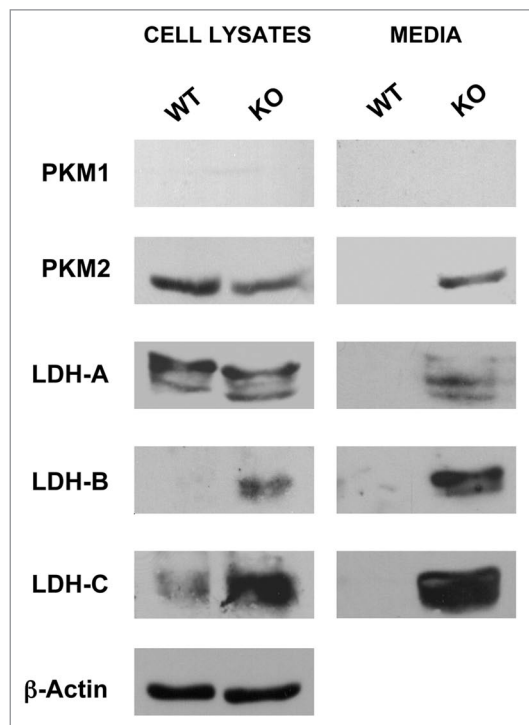


Figure 6. Validation of the upregulation of PKM2 and LDH isoforms in Cav-1 (-/-) deficient fibroblasts. Media and cell lysates were prepared from WT and Cav-1-deficient stromal fibroblasts, and subjected to SDS-PAGE and western blot analysis with anti-PKM1/2 or anti-LDH isoform-specific antibodies. Note the upregulation of PKM2, and LDH-A, B and C in the tissue culture media harvested from Cav-1-deficient cells. Also, note the upregulation of LDH-B and LDH-C in Cav-1 deficient cell lysates.

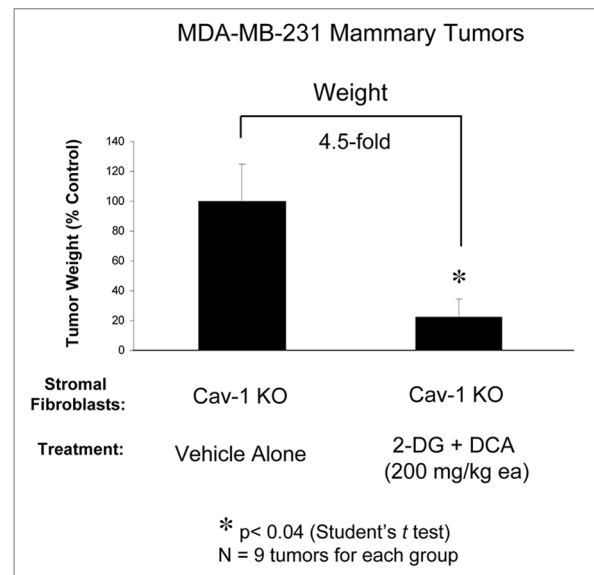


Figure 7. Treatment with glycolysis inhibitors functionally blocks cancer-associated fibroblast induced breast cancer tumor growth. Based on our unbiased proteomics studies, the Warburg effect in the myo-fibroblast compartment may be a key factor driving tumor growth. To test this hypothesis directly, mice co-injected with Cav-1-deficient stromal fibroblasts and MDA-MB-231 breast cancer cells were treated with glycolysis inhibitors. For this purpose, we tested the efficacy of two well-established glycolysis inhibitors, namely 2-DG (2-deoxy-D-glucose) and DCA (dichloro-acetate), individually or in combination. Individually 2-DG or DCA had no effect on tumor growth at a dosage of 200 mg/kg (not shown). However, 2-DG and DCA, used in combination, dramatically reduced tumor growth that was dependent on Cav-1-deficient stromal fibroblasts. Note that we observed a striking 4.5-fold reduction in tumor mass, as predicted.

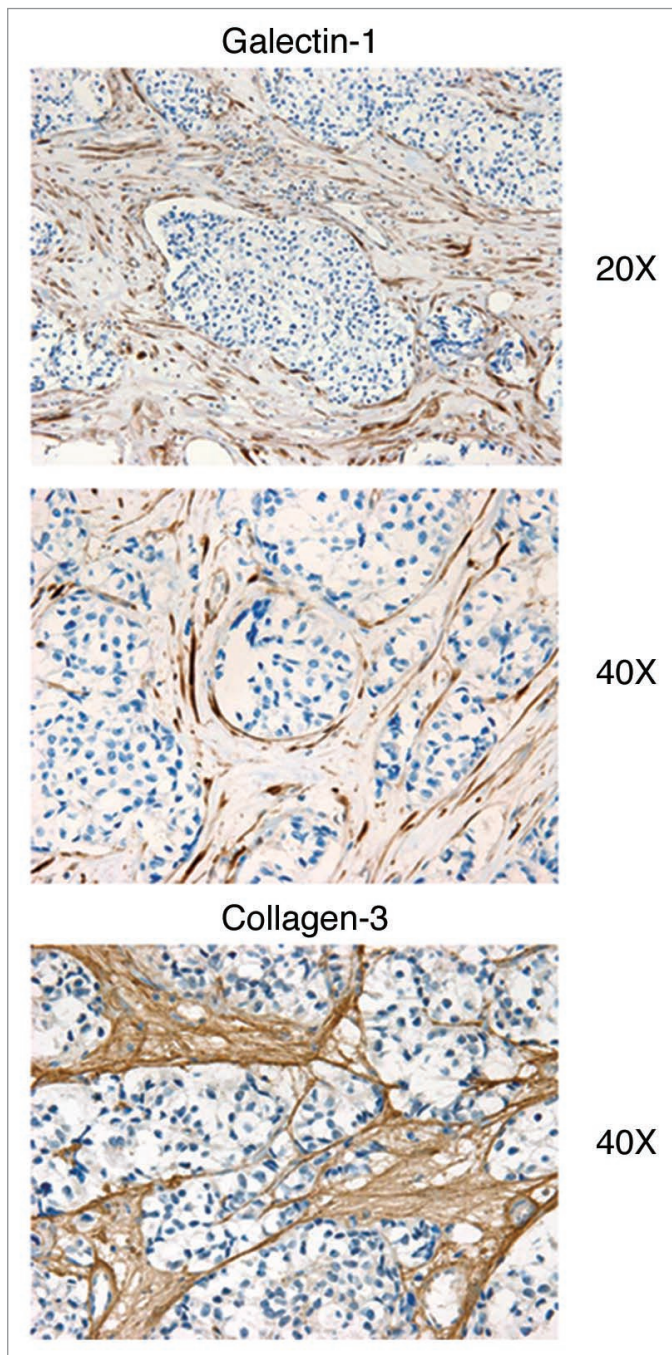


Figure 8. Expression of extracellular matrix proteins, Galectin-1 and Collagen-3, in breast cancers that lack stromal Cav-1 expression. Paraffin-embedded tissue sections from human breast cancer samples were immuno-stained with antibodies directed against galectin-1 and collagen-3. Slides were counterstained with hematoxylin. Note that breast cancer tumor sections show the overexpression of galectin-1 and collagen 3, in the tumor stromal compartment. Also, note that tumor cell 'nests' surrounded by positively-stained stroma were observed. Original magnification, 20X and 40X, as indicated.

Cav-1.¹¹ Then, these Cav-1 deficient cancer-associated fibroblasts could “feed” adjacent tumor epithelial cells by the secretion of energy-rich metabolites, such as pyruvate and lactate, that then would enter the TCA cycle (oxidative phosphorylation) in the

epithelial cancer cells. We have previously termed this new idea the “Reverse Warburg Effect,”¹¹ because the “Warburg effect” was thought to be confined to epithelial cancer cells, and not to the tumor stroma. This new hypothesis was largely based on the unbiased proteomic and transcriptional analysis of primary cultures of mesenchymal stem cells (bone marrow stromal cells) derived from Cav-1 (-/-) deficient mice, a new genetic “myofibroblast” model of cancer-associated fibroblasts.¹¹

Here, we show for the first time that immortalized Cav-1 (-/-) deficient fibroblasts are pro-tumorigenic in vivo, and are indeed sufficient to promote tumor neovascularization, via the recruitment of Cav-1 (+) microvascular cells. Importantly, these immortalized Cav-1 (-/-) deficient fibroblasts also showed a proteomic shift towards aerobic glycolysis, consistent with the “Reverse Warburg Effect.” In accordance with these findings, energy restriction with glycolysis inhibitors (2-DG and DCA) was sufficient to block the tumor growth stimulated by Cav-1 (-/-) deficient fibroblasts.

We also showed that glycolytic enzymes (such as PKM2 and LDH-B) are selectively upregulated in the fibroblastic stromal compartment of human breast cancer samples that lack stromal Cav-1 expression. As such, stromal PKM2 and LDH-B may be novel biomarkers for the “Reverse Warburg Effect,” allowing the stratification and selection of breast cancer patients for metabolic-based therapies.

Our previous studies using PKM2 isoform-specific antibodies also localized PKM2 to the breast cancer tumor stroma, using two different mouse monoclonal antibodies (from ScheBo Biotech and Abcam).¹¹ Here, we used two newly-released rabbit polyclonal antibodies (from Proteintech, Inc. and Cell Signaling Technology, Inc.) directed against the specific protein sequence of the exon that is unique to PKM2, and we obtained similar results. Thus, using four distinct antibody probes, we can now localize PKM2 to the tumor stromal compartment in human breast cancer patients that lack stromal Cav-1 expression. Importantly, the localization of PKM2 was previously thought to be confined only to epithelial cancer cells undergoing the Warburg effect.

Consistent with the stromal localization of PKM2, we also observed the striking localization of LDH-B in the myofibroblastic tumor stromal compartment. Other LDH isoforms (LDH-A and LDH-C) were present in both the tumor epithelial and stromal compartments. Thus, the tumor stromal expression of PKM2 and LDH-B may be critical to mediate the “Reverse Warburg Effect,” leading to poor clinical outcome in human breast cancer patients. Future biomarker and mechanistic studies will be necessary to test this hypothesis directly.

Interestingly, we observed that PKM2 and LDH isoforms were also present in the cell culture media derived from Cav-1 (-/-) deficient stromal fibroblasts. Similarly, autocrine motility factor (AMF), which is identical to glucose-6-phosphate isomerase (GPI), is an essential glycolytic enzyme that is secreted and increases the motility and metastatic capacity of cancer cells.¹⁷ Perhaps extracellular PKM2 and LDH may serve a similar function. Alternatively, the secretion of glycolytic enzymes by cancer associated fibroblasts could allow glycolysis

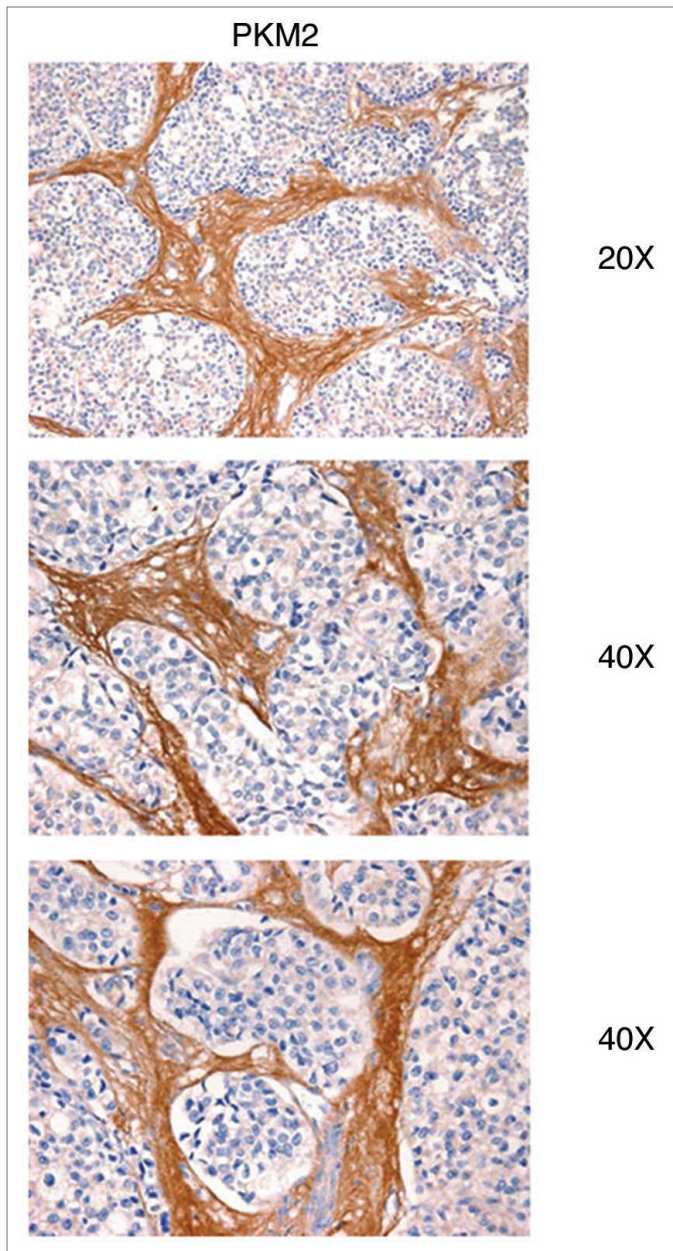


Figure 9. Extracellular matrix expression of pyruvate kinase (M2-isoform) in human breast cancers that lack stromal Cav-1 expression. Paraffin-embedded tissue sections from human breast cancer samples were immuno-stained with isoform-specific affinity-purified antibodies directed against PKM2 (from Proteintech Group, Inc.). Slides were counterstained with hematoxylin. Note that breast cancer tumor sections show the overexpression of PKM2 in the tumor extracellular matrix compartment. Tumor cell 'nests' surrounded by PKM2 positively-stained matrix were observed. Original magnification, 20X and 40X, as indicated.

to take place outside the cell in the tumor microenvironment, or even at the cell surface of cancer cells undergoing oxidative phosphorylation.

In accordance with our current findings, several recent reports¹⁸⁻²² have now suggested that cancer cells may show a preference for oxidative phosphorylation (not aerobic glycolysis), and

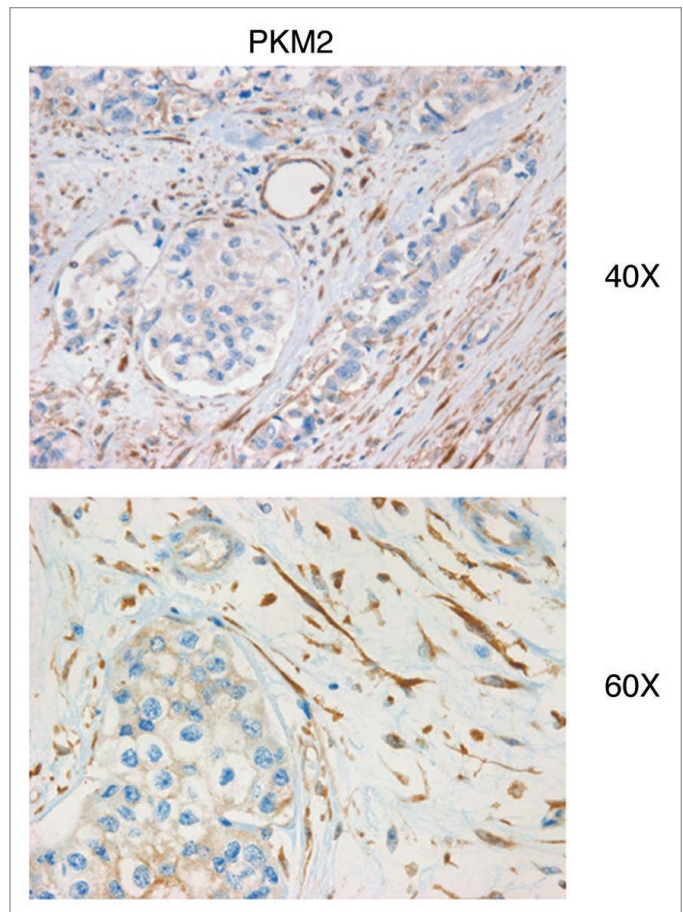


Figure 10. Stromal fibroblast expression of pyruvate kinase (M2-isoform) in human breast cancers that lack stromal Cav-1 expression. Paraffin-embedded tissue sections from human breast cancer samples were immuno-stained with isoform-specific affinity-purified antibodies directed against PKM2 (from Cell Signaling Technology, Inc.). Slides were counterstained with hematoxylin. Note that breast cancer tumor sections show the overexpression of PKM2 in the fibroblastic tumor stromal compartment. Tumor cell 'nests' surrounded by PKM2 positively-stained stromal fibroblasts were observed. Original magnification, 40X, and 60X, as indicated.

that this correlates with their capacity for increased tumor growth and metastasis. These findings also directly support the "Reverse Warburg Hypothesis" or more generally "Stromal-Epithelial Metabolic Coupling" (summarized in Fig. 13).

We have previously shown that the predictive value of a loss of stromal Cav-1 in human breast cancer patients is independent of epithelial marker status.^{4,5,7} As such, a loss of stromal Cav-1 has strong prognostic value in all the different epithelial subtypes of human breast cancer, including triple-negative breast cancer patients and DCIS patients.^{4,5,7}

Here, we used the aggressive and highly metastatic human breast cancer cell line, namely MDA-MB-231 cells, that is derived from a pleural effusion. These cells have been extensively characterized and have been classified as a basal-like triple-negative breast cancer cell line. Thus, our current stromal studies with chemically-induced metabolic restriction (using glycolysis inhibitors) may have new implications for the therapy of triple-negative

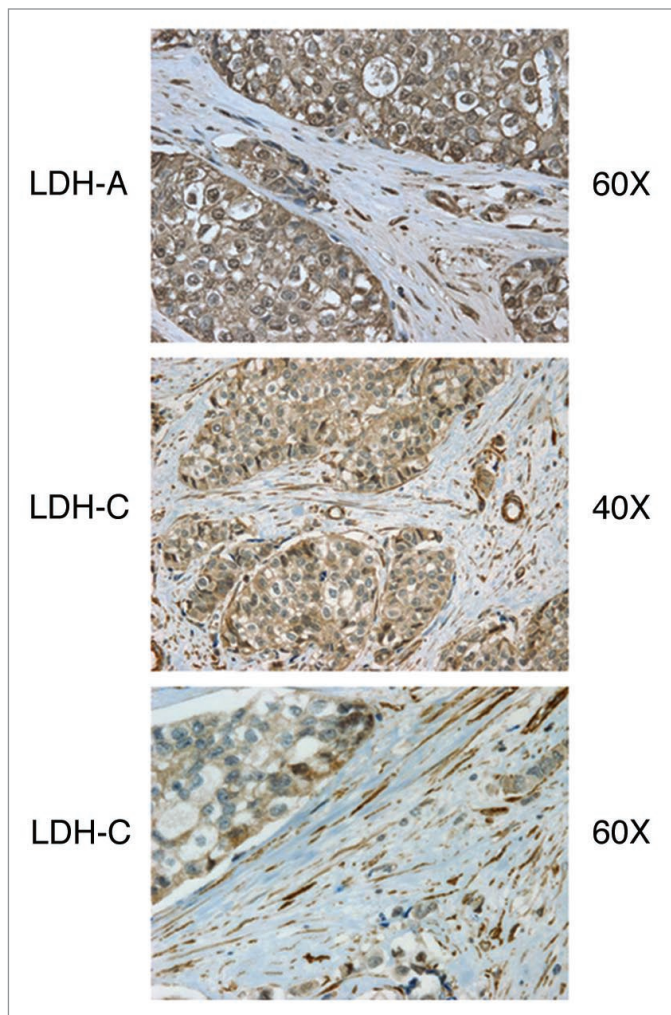


Figure 11. LDH isoforms (-A and -C) are overexpressed in the stroma of human breast cancers that lack stromal Cav-1 expression. Paraffin-embedded tissue sections from human breast cancer samples were immuno-stained with isoform-specific antibodies directed against LDH-A and LDH-C. Slides were counterstained with hematoxylin. Note that LDH-A and LDH-C isoforms were localized in both the breast cancer tumor epithelial cells and the fibroblastic stromal compartment, with LDH-C showing some preference for the stromal compartment. Original magnification, 40X, and 60X, as indicated.

breast cancer patients, as well as all the other epithelial subclasses of human breast cancer, including DCIS lesions.

Materials and Methods

Materials. Antibodies for immuno-staining and Western blotting were obtained from commercial sources: anti-galectin-1 (LGALS1) (#HPA000646; Sigma); anti-collagen-3 (#ab7778; Abcam, Inc.); anti-LDH-A (#SAB1100050; Sigma); anti-LDH-B (#AV48210 and #WH0003945M1; Sigma); anti-LDH-C (#SAB1100051; Sigma); anti-PKM1 (#15821-1-AP/SR; Proteintech Group, Inc.); anti-PKM2 (#15822-1-AP/SR; Proteintech Group, Inc.); anti-PKM2 (#3198S; Cell Signaling Technology, Inc.). 2-DG (2-deoxy-D-glucose) and

DCA (dichloro-acetate) were purchased from Sigma-Aldrich. 2-DG is a glycolysis inhibitor, while DCA is a more specific inhibitor of aerobic glycolysis, which prevents lactate accumulation. MDA-MB-231 cells were obtained from ATCC. The Streptavidin-HRP kit was from Dako (Carpinteria, CA).

Origin and derivation of immortalized Cav-1 (-/-) deficient fibroblasts. Mouse embryo fibroblasts (MEFs) were immortalized, as we previously described.^{23,24} First, Cav-1 (-/-) deficient mice were crossed into the genetic background of Ink4a (-/-) mice, to facilitate cell immortalization (all in the C57Bl/6 background). Then, MEFs were prepared from both Cav-1 (+/+)/Ink4a (-/-) mice and Cav-1 (-/-)/Ink4a (-/-) mice, and transduced with a retroviral vector encoding v-Src (pBABE-v-Src-puro).²³ For simplicity, these cells are referred to throughout the text as immortalized WT and Cav-1 (-/-) deficient stromal fibroblasts. Importantly, we have previously shown that these 2 fibroblast cell lines express equivalent amounts of v-Src by Western blot analysis.²³ Virtually identical results were also obtained with Cav-1 (+/+) and Cav-1 (-/-) fibroblasts in the Ink4a (-/-) background that were transduced with a retroviral vector encoding PyMT (pBABE-PyMT-puro). In this case, these PyMT-immortalized Cav-1 (-/-) fibroblasts conferred an 8.7-fold increase in mammary tumor mass, relative to PyMT-immortalized Cav-1 (+/+) fibroblasts (Suppl. Fig. 3).

Animal studies. All animals were housed and maintained in a pathogen-free environment/barrier facility at the Kimmel Cancer Center at Thomas Jefferson University under National Institutes of Health (NIH) guidelines. Mice were kept on a 12-hour light/dark cycle with ad libitum access to chow and water. Approval for all animal protocols used for this study was review and approved by the Institutional Animal Care and Use Committee (IACUC). Briefly, a mixture of tumor cells (MDA-MB-231; 1×10^6 cells) plus fibroblasts (3×10^5 cells) in 100 μ l of sterile PBS were co-injected into the flanks of athymic NCr nude mice (NCRNU; Taconic Farms; 6–8 weeks of age). Mice were then sacrificed at 2 weeks post-injection; tumors were excised to determine their weight and size using calipers. The formula $(X^2Y)/2$, where X is the width and Y is the length, was also used in order to estimate tumor volume. In complementary experiments employing glycolysis inhibitors, 2-DG (2-deoxy-glucose; 200 mg/kg/mouse) and DCA (dichloro-acetate; 200 mg/kg/mouse) were dissolved and administered in sterile PBS using a total volume of 100 μ l per injection. The injection of these drugs was performed intraperitoneally (I.P.), every other day, over a period of 2 weeks. Vehicle alone (PBS) was injected in control mice.

Quantitation of tumor angiogenesis. Immunohistochemical staining with CD31 antibody was performed on frozen tumor sections. For the detection, a three-step biotin-streptavidin-horseradish peroxidase method was employed. Frozen tissue sections (6 μ m) were fixed in acetone at -20°C for 5 min and air dried. After blocking with 10% rabbit serum the sections were incubated overnight at 4°C with rat anti-mouse CD31 antibody at a dilution of 1:200, followed by biotinylated rabbit anti-rat IgG (1:200) antibody and streptavidin-HRP. Immunoreactivity was revealed with 3,3'-diaminobenzidine. For quantitation of CD31-positive vessels, images were captured of one 20x field

from the central region of each tumor section representing an area of 0.56 mm² or 560,000 μm.² The total number and area of each vessel was calculated using Image J and the data was represented graphically. Immunodetection of Cav-1 was performed on tumor paraffin sections. Briefly, sections were deparaffinized, rehydrated through graded ethanols and washed in PBS. Antigen retrieval was performed in 0.01 M citrate buffer, pH 6.0 for 10 minutes using an electric pressure cooker. The sections were cooled to room temperature, blocked with 3% H₂O₂ for 10 min and then with 10% goat serum in PBS. The sections were incubated overnight at 4°C with rabbit anti-Cav-1 IgG (N-20; Santa Cruz Biotech, Inc.,) at a dilution of 1:1,000. After washing in PBS, the sections were incubated with a biotinylated goat anti-rabbit IgG, followed by a streptavidin-HRP conjugate (Dako, Carpinteria, CA).

Immunofluorescence microscopy. Frozen tissue sections (6 μm) were fixed in acetone at -20°C for 5 min and air dried. After blocking with 10% goat serum the sections were incubated overnight at 4°C with rat anti-mouse CD31 antibody at a dilution of 1:100, followed by the incubation with the secondary antibody donkey anti-rat (1:1,000), rhodamine conjugated, for 30 minutes at room temperature. Finally, sections were washed three times with PBS (10 minutes each wash), and mounted on a glass slide with slow-fade anti-fade reagent (Molecular Probes, Eugene, OR). Fluorescent DNA-intercalating dye 4,6-diamidino-2-phenylindole (DAPI) staining nuclei was also performed. GFP(+) tumor cells and their surrounding vasculature were visualized using this approach.

Preparation of “conditioned media” from Cav-1 (-/-) deficient fibroblasts. Immortalized WT and Cav-1 (-/-) fibroblasts were cultured in normal medium until they reached confluence. Then, the cells were washed 3 times with PBS and cultured in DMEM (supplemented with 0.1% Nu-Serum IV (BD Biosciences; #355104)). After 48 hours, tissue culture supernatants were collected, filtered through a 0.45 μm pore filter, and concentrated by Centriprep YM-10 (Millipore), according to the manufacturer’s instructions. Concentrated samples were stored at -80°C until proteomic analysis.

Proteomic analysis. 2-D DIGE (two-dimensional difference gel electrophoresis)²⁵ and mass spectrometry protein identification were run by Applied Biomics (Hayward, CA). Image scans were carried out immediately following the SDS-PAGE using Typhoon TRIO (Amersham BioSciences) following the protocols provided. The scanned images were then analyzed by Image QuantTL software (GE-Healthcare), and then subjected to in-gel analysis and cross-gel analysis using DeCyder software version 6.5 (GE-Healthcare). The ratio of protein differential expression was obtained from in-gel DeCyder software analysis. The selected spots were picked by an Ettan Spot Picker (GE-Healthcare) following the DeCyder software analysis and spot picking design. The selected protein spots were subjected to in-gel trypsin digestion, peptides extraction, desalting and followed by MALDI-TOF/TOF (Applied Biosystems) analysis to determine the protein identity.

Immunoblot analysis. Media samples and cell lysates were prepared from WT and Cav-1 (-/-) stromal fibroblasts to validate

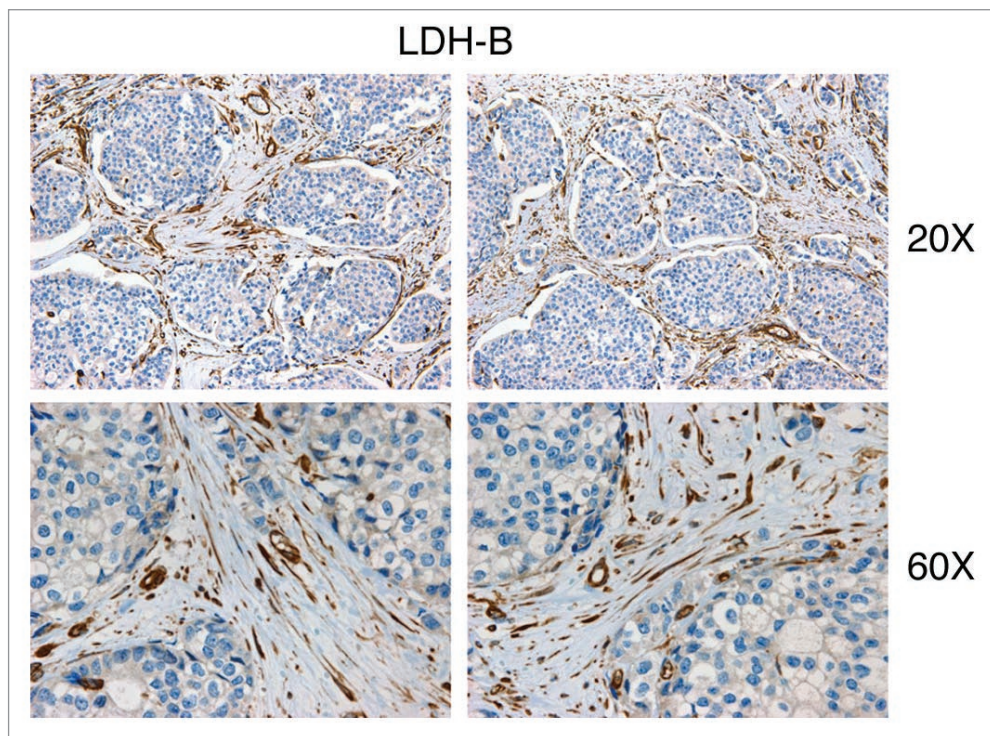


Figure 12. LDH-B is highly and selectively expressed in the breast cancer tumor stroma. Paraffin-embedded tissue sections from human breast cancer samples were immuno-stained with antibodies directed against LDH-B. Slides were counterstained with hematoxylin. Note that breast cancer tumor sections show the overexpression of LDH-B selectively in the tumor stromal compartment. Tumor cell ‘nests’ surrounded by LDH-B positively-stained stromal fibroblasts were observed. Original magnification, 20X, and 60X, as indicated.

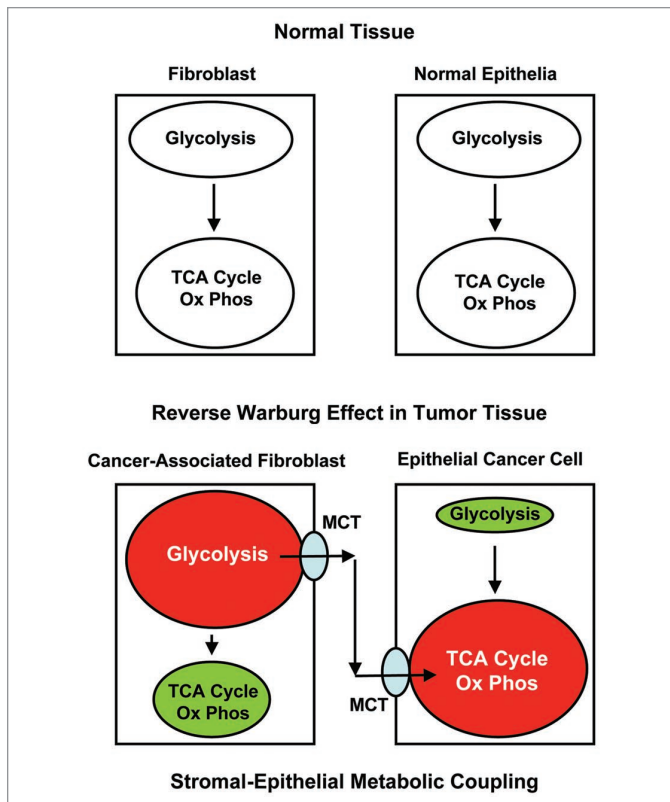


Figure 13. The 'Reverse Warburg Effect': Stromal-epithelial metabolic coupling in the tumor microenvironment. Upper, normal tissue. We postulate that in normal tissue there is a lack of metabolic coupling between fibroblasts and normal epithelial cells. Lower, the reverse Warburg effect in tumor tissue. We propose that stromal-epithelial metabolic coupling occurs between cancer-associated fibroblasts and epithelial cancer cells. In this scenario, cancer-associated fibroblasts would show a shift towards aerobic glycolysis (highlighted in red) and the epithelial cancer cells would show a shift towards oxidative metabolism (highlighted in red). Thus, energy-rich metabolites (such as pyruvate and lactate) produced and secreted from cancer-associated fibroblasts, could then enter the TCA cycle and undergo oxidative metabolism in adjacent epithelial cancer cells, thereby promoting tumor growth. In essence, the cancer-associated fibroblasts would 'feed' the tumor cells. MCT, mono-carboxylate transporters; Ox Phos, oxidative phosphorylation. The activity of metabolic pathways shown in red is increased and those shown in green is reduced.

our results from proteomics analysis by western blot analysis. Briefly, cells were collected by cell scraping after washing with PBS, passed several times through a 26-gauge needle to completely disrupt all cells, using an appropriate volume of lysis buffer (10 mM Tris, pH 7.5, 150 mM NaCl, 1% Triton X-100 and 60 mM *n*-octyl-glucoside), containing protease inhibitors (Boehringer Mannheim, Indianapolis, IN). Cell lysates were then centrifuged at 12,000 xg for 10 minutes (at 4°C) to remove insoluble debris. Protein concentrations were analyzed using the BCA reagent (Pierce, Rockford, IL). Samples were then separated by SDS-PAGE (10% acrylamide) and transferred to nitrocellulose. All subsequent wash buffers contained 10 mM Tris, pH 8.0, 150 mM NaCl, 0.05% Tween 20, which was supplemented with 5% nonfat dry milk (Carnation) for the blocking solution,

and 1% bovine serum albumin for the antibody diluent. Primary antibodies directed against LDHA, B and C were used at a 1:500 dilution. PKM2 antibodies were used at a dilution of 1:1,000. Horseradish peroxidase-conjugated secondary antibodies were used to visualize bound primary antibodies with the Supersignal chemiluminescence substrate (Pierce, Rockford, IL).

Immuno-histochemical analysis of human breast cancer samples. Immunohistochemical staining was performed essentially as we previously described.^{5,7} Briefly, 5- μ m sections from paraffin-embedded breast cancer tissue were de-paraffinized and rehydrated by passage through a graded series of ethanol. Antigen retrieval was performed by heating the slides in 10 mM sodium citrate buffer, pH 6.0, for 10 minutes using a pressure cooker. Endogenous peroxidase activity was quenched with 3% H₂O₂ for 10 minutes. Then, slides were washed with phosphate-buffered saline (PBS) and blocked with 10% goat serum in PBS for 1 hour at room temperature. Samples were incubated with the primary antibodies diluted in 1% BSA in PBS overnight at 4°C. After washing in PBS (three times, 5 minutes each), slides were stained with the LSAB2 system kit (Dako Cytomation, Glostrup, Denmark), according to the manufacturer's recommendations. Briefly, samples were incubated with biotinylated linker antibodies for 30 minutes, washed in PBS (three times, 5 minutes each), and then incubated with a streptavidin-horseradish peroxidase-conjugated solution for 30 minutes. After washing, samples were incubated with the diaminobenzidine reagent until color production developed. Finally, the slides were rinsed with tap water and counter-stained with hematoxylin, dehydrated, and mounted with coverslips. Importantly, critical negative controls were performed in parallel for all of the immunohistochemical studies.

Statistical analysis. Statistical significance was examined using the Student's *t*-test. Values of $p < 0.05$ were considered significant. Values were expressed as means \pm SEM.

Acknowledgements

M.P.L. and his laboratory were supported by grants from the NIH/NCI (R01-CA-080250; R01-CA-098779; R01-CA-120876; R01-AR-055660) and the Susan G. Komen Breast Cancer Foundation. A.K.W. was supported by a Young Investigator Award from Breast Cancer Alliance, Inc. and a Susan G. Komen Career Catalyst Grant. F.S. was supported by grants from the W.W. Smith Charitable Trust, the Breast Cancer Alliance (BCA) and a Research Scholar Grant from the American Cancer Society (ACS). P.G.F. was supported by a grant from the W.W. Smith Charitable Trust and a Career Catalyst Award from the Susan G. Komen Breast Cancer Foundation. R.G.P. was supported by grants from the NIH/NCI (R01-CA-70896, R01-CA-75503, R01-CA-86072 and R01-CA-107382) and the Dr. Ralph and Marian C. Falk Medical Research Trust. The Kimmel Cancer Center was supported by the NIH/NCI Cancer Center Core grant P30-CA-56036 (to R.G.P.). Funds were also contributed by the Margaret Q. Landenberger Research Foundation (to M.P.L.).

This project is funded, in part, under a grant with the Pennsylvania Department of Health (to M.P.L.). The Department

specifically disclaims responsibility for any analyses, interpretations or conclusions. We also thank Dr. Gabriela Dontu (U.K.) for her critical suggestions.

References

1. Ronnov-Jessen L, Bissell MJ. Breast cancer by proxy: can the microenvironment be both the cause and consequence? *Trends Mol Med* 2009; 15:5-13.
2. Ghajar CM, Meier R, Bissell MJ. Quis custodiet ipsos custodiet: who watches the watchmen? *Am J Pathol* 2009; 174:1996-9.
3. Mercier I, Casimiro MC, Wang C, Rosenberg AL, Quong J, Allen KG, et al. Human breast cancer-associated fibroblasts (CAFs) show caveolin-1 downregulation and RB tumor suppressor functional inactivation: Implications for the response to hormonal therapy. *Cancer Biol Ther* 2008; 7:1212-25.
4. Witkiewicz AK, Casimiro MC, Dasgupta A, Mercier I, Wang C, Bonuccelli G, et al. Towards a new "stromal-based" classification system for human breast cancer prognosis and therapy. *Cell Cycle* 2009; 8:1654-8.
5. Witkiewicz AK, Dasgupta A, Sotgia F, Mercier I, Pestell RG, Sabel M, et al. An absence of stromal caveolin-1 expression predicts early tumor recurrence and poor clinical outcome in human breast cancers. *Am J Pathol* 2009; 174:2035-34.
6. Sloan EK, Ciocca D, Pouliot N, Natoli A, Restall C, Henderson M, et al. Stromal cell expression of caveolin-1 predicts outcome in breast cancer. *Am J Pathol* 2009; 174:2035-43.
7. Witkiewicz AK, Dasgupta A, Nguyen KH, Liu C, Kovatich AJ, Schwartz GF, et al. Stromal caveolin-1 levels predict early DCIS progression to invasive breast cancer. *Cancer Biol Ther* 2009; 8:1167-75.
8. Di Vizio D, Morello M, Sotgia F, Pestell RG, Freeman MR, Lisanti MP. An absence of stromal caveolin-1 is associated with advanced prostate cancer, metastatic disease and epithelial Akt activation. *Cell Cycle* 2009; 8:2420-4.
9. Williams TM, Sotgia F, Lee H, Hassan G, Di Vizio D, Bonuccelli G, et al. Stromal and epithelial caveolin-1 both confer a protective effect against mammary hyperplasia and tumorigenesis: Caveolin-1 antagonizes cyclin D1 function in mammary epithelial cells. *Am J Pathol* 2006; 169:1784-801.
10. Sotgia F, Del Galdo F, Casimiro MC, Bonuccelli G, Mercier I, Whitaker-Menezes D, et al. Caveolin-1^{-/-} null mammary stromal fibroblasts share characteristics with human breast cancer-associated fibroblasts. *Am J Pathol* 2009; 174:746-61.
11. Pavlides S, Whitaker-Menezes D, Castello-Cros R, Flomenberg N, Witkiewicz AK, Frank PG, et al. The reverse Warburg effect: aerobic glycolysis in cancer associated fibroblasts and the tumor stroma. *Cell Cycle* 2009; 8:3984-4001.
12. King MP, Attardi G. Human cells lacking mtDNA: repopulation with exogenous mitochondria by complementation. *Science* 1989; 246:500-3.
13. Yi CH, Smith DJ, West WW, Hollingsworth MA. Loss of fibulin-2 expression is associated with breast cancer progression. *Am J Pathol* 2007; 170:1535-45.
14. Jung EJ, Moon HG, Cho BI, Jeong CY, Joo YT, Lee YJ, et al. Galectin-1 expression in cancer-associated stromal cells correlates tumor invasiveness and tumor progression in breast cancer. *Int J Cancer* 2007; 120:2331-8.
15. van den Brule FA, Waltregny D, Castronovo V. Increased expression of galectin-1 in carcinoma-associated stroma predicts poor outcome in prostate carcinoma patients. *J Pathol* 2001; 193:80-7.
16. Vander Heiden MG, Cantley LC, Thompson CB. Understanding the Warburg effect: the metabolic requirements of cell proliferation. *Science* 2009; 324:1029-33.
17. Funasaka T, Hogan V, Raz A. Phosphoglucose isomerase/autocrine motility factor mediates epithelial and mesenchymal phenotype conversions in breast cancer. *Cancer Res* 2009; 69:5349-56.
18. Reich NC. STAT3 revs up the powerhouse. *Sci Signal* 2009; 2:61.
19. Gough DJ, Corlett A, Schlessinger K, Wegrzyn J, Larner AC, Levy DE. Mitochondrial STAT3 supports Ras-dependent oncogenic transformation. *Science* 2009; 324:1713-6.
20. Wegrzyn J, Potla R, Chwae YJ, Sepuri NB, Zhang Q, Koek T, et al. Function of mitochondrial Stat3 in cellular respiration. *Science* 2009; 323:793-7.
21. Dang CV. p32 (C1QBP) and Cancer Cell Metabolism: Is the Warburg Effect a lot of hot air? *Mol Cell Biol* 2010; 30:1300-2.
22. Fogal V, Richardson A, Karmali PP, Scheffler IE, Smith JW, Ruoslahti E. Mitochondrial p32 protein is a critical regulator of tumor metabolism via maintenance of oxidative phosphorylation. *Mol Cell Biol* 2010.
23. Williams TM, Lee H, Cheung MW, Cohen AW, Razani B, Iyengar P, et al. Combined loss of INK4a and caveolin-1 synergistically enhances cell proliferation and oncogene-induced tumorigenesis: Role of INK4a/CAV-1 in mammary epithelial cell hyperplasia. *J Biol Chem* 2004; 279:24745-56.
24. Williams TM, Medina F, Badano I, Hazan RB, Hutchinson J, Muller WJ, et al. Caveolin-1 gene disruption promotes mammary tumorigenesis and dramatically enhances lung metastasis in vivo: Role of Cav-1 in cell invasiveness and matrix metalloproteinase (MMP-2/9) secretion. *J Biol Chem* 2004; 279:51630-46.
25. Marouga R, David S, Hawkins E. The development of the DIGE system: 2D fluorescence difference gel analysis technology. *Anal Bioanal Chem* 2005; 382:669-78.

Note

Supplementary materials can be found at: www.landesbioscience.com/supplement/BonuccelliCC9-10-Sup.pdf